

Transport properties of $\text{Ti}_2\text{Ba}_2\text{CaCu}_2\text{O}_8$ weak links on LaAlO_3 bicrystal substrates

Y. F. Chen,^{a)} Z. G. Ivanov,^{b)} E. A. Stepanov,^{c)} A. Ya. Tzalenchuk,^{c)} S. Zarembinski,^{d)} and T. Claeson

Department of Physics, Chalmers University of Technology and University of Göteborg, S-412 96 Göteborg, Sweden

L.-G. Johansson

Department of Inorganic Chemistry, University of Göteborg, S-412 96 Göteborg, Sweden

(Received 20 November 1995; accepted for publication 19 February 1996)

Josephson junctions and dc superconducting quantum interference devices (SQUIDs) have been fabricated in *ex situ* epitaxial $\text{Ti}_2\text{Ba}_2\text{CaCu}_2\text{O}_8$ films on bicrystal LaAlO_3 substrates with symmetric 32° [001] tilt grain boundaries. The critical temperature T_c , of the junctions was in the range 105–107 K and the critical current densities at 77 K varied between 3×10^2 and 3×10^4 A/cm², two or three orders of magnitude less than those of the film. The I - V curves are described by a resistively shunted junction model. Close to T_c , the temperature dependence of the critical current was described by $(1 - T/T_c)^2$. The flux noise spectra $S_\Phi(f)$ of dc SQUIDs were measured in the locked-loop regime with constant current bias at temperatures up to 94 K. The white noise level was $50 \mu\Phi_0 / \sqrt{\text{Hz}}$ at 77 K. The crossover frequency to $1/f$ noise was low, about 5 Hz, and the flux noise level at 1 Hz was $440 \mu\Phi_0 / \sqrt{\text{Hz}}$. © 1996 American Institute of Physics. [S0021-8979(96)01411-1]

I. INTRODUCTION

Grain boundaries in high- T_c superconductors (HTSs) play a very important role in the formation of Josephson junctions. Artificial grain boundaries exhibiting the Josephson effect in HTS thin films may be produced using either the bicrystal substrate,¹ the step edge,² or the biepitaxial process.³ Compared with other types of grain-boundary structures, the bicrystal structure is straightforward to prepare and is relatively well understood. In the last several years, many competitive results have been reported on bicrystal and step-edge Josephson junctions in $\text{YBa}_2\text{Cu}_3\text{O}_{7-\delta}$ (YBCO) thin films. TI-based films show higher critical temperature T_c , 110–125 K, other parameters being comparable to those of YBCO and BiSCCO films.⁴ The low-noise performance of the first $\text{Ti}_2\text{Ba}_2\text{CaCu}_2\text{O}_8$ (TI-2212) dc superconducting quantum interference devices (SQUIDs)^{5,6} was promising and stimulated further experiments. In this article we present and discuss results obtained on TI-2212 Josephson junctions and dc SQUIDs on LaAlO_3 (LAO) bicrystal substrates.

II. DEVICE PREPARATION

The choice of a 32° angle grain boundary in our investigations was based on our previous experiments with YBCO,⁷ and TI-2212,⁸ bicrystal junctions. The LAO bicrystal substrates were produced by the solid-phase intergrowing method.⁹ The TI-2212 films were epitaxially grown by an

situ method presented elsewhere.¹⁰ Shortly, an amorphous precursor film was deposited on a bicrystal LAO substrate by pulsed laser ablation of a carbonate-free target with a nominal composition $\text{Ba}_2\text{CaCu}_2\text{O}_x$. The oxygen pressure was 2×10^{-2} mbar and the deposition rate was 0.4 \AA pulse. The precursor film was sealed inside a TI-2212 crucible and annealed in Ti_2O atmosphere at high temperature. Films prepared under optimal conditions have T_c varying from 105–109 K, the width of transition being 1–2 K. The films were epitaxial, c -axis oriented, with smooth background and small areas with trellislike structure. Φ scan indicated the absence of high-angle grain boundaries and the rocking curve has a full width at half-maximum (FWHM) of 0.37° .¹¹ The film thickness was about 300 nm.

Microbridges and dc SQUIDs were patterned by photolithography and Ar-ion-beam milling. Two microbridges, 5 and 10 μm wide, and a dc SQUID consisting of two 5- μm -wide microbridges in a $20 \times 20 \mu\text{m}^2$ loop crossed the grain boundary of the chip. In addition, two 5- μm -wide microbridges were placed on each half of the bicrystal to control the intragrain critical current density (see insert in Fig. 2). After patterning, T_c was reduced by 1–2 K and the transition obtained a long tail (see the insert in Fig. 1). The dc SQUIDs were measured in a screened environment, using μ -metal and Nb superconducting shields.

III. RESULTS AND DISCUSSION

Figure 2 shows the I - V characteristic of a TI-2212 bicrystal junction. The I - V curve exhibited RSJ-model behavior without hysteresis. Close to T_c the I - V curves were rounded by thermal noise and flux motion. The critical currents of the junctions were determined using a voltage criterion of 1 μV with no account for the rounding of the I - V curves at high temperatures.

^{a)}Permanent address: National Laboratory for Superconductors, Institute of Physics, Chinese Academy of Sciences, 100080 Beijing, People's Republic of China.

^{b)}Electronic mail: f4azi@fy.chalmers.se

^{c)}Institute of Crystallography, Russian Academy of Sciences, 117333 Moscow, Russia.

^{d)}Institute of Physics, Polish Academy of Sciences, Warsaw, Poland.

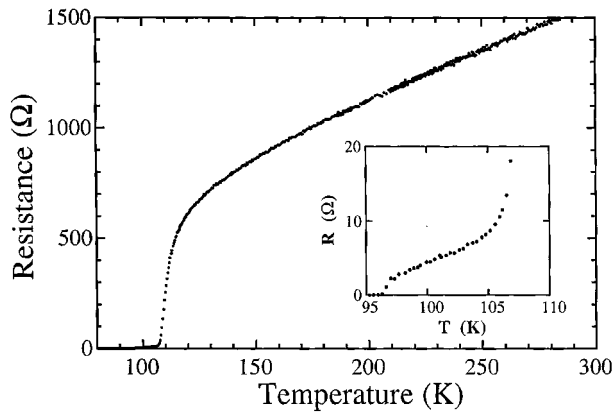


FIG. 1. The temperature dependence of the resistance of a TI-2212 bicrystal junction on a LAO substrate. The insert shows the long tail in the transition region.

The temperature dependence of the normalized critical current (I_c/I_{c0} , I_{c0} being the critical current at 4.2 K) is shown in Fig. 3 for three junctions (J_1 , J_2 , and J_3 all on one chip). The critical temperatures of the junctions $T_c=105$, 105.5, and 104.8 K, critical current densities at 77 K $I_c=6\times 10^3$, 4×10^3 , and 2×10^4 A/cm², and characteristic voltage at 77 K $I_c R_n=56$, 40, and 22 μ V, respectively. Close to T_c , the temperature dependence of the normalized critical current can be described as $(1-T/T_c)^2$, while at low temperature it is proportional to $(1-T/T_c)$. The normal resistance R_n decreases with decreasing the temperature and reaches a constant value at low temperature (see the insert in Fig. 3 showing R_n as a function of T/T_c for the junction J_3). This decrease in R_n with T is stronger than that observed for YBCO bicrystal junctions.¹² The temperature dependencies of both I_c and R_n suggest that the junctions behave as superconductor-normal-metal-superconductor (SNS) weak links. The critical current densities and the normal resistances for these bicrystal junctions were comparable to those presented in Ref. 13.

The critical currents of the junctions vary with magnetic field with a maximum depression of 75% at 77 K.

The ac Josephson effect under external microwave radiation at 77 K is shown in Fig. 4(a) at different levels of mi-

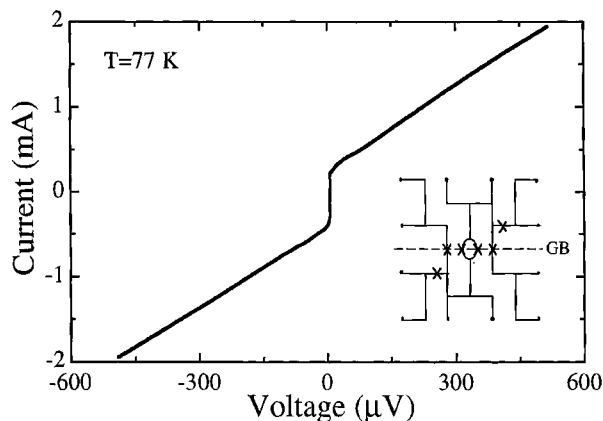


FIG. 2. I - V characteristic of the TI-2212 bicrystal junction on a LAO substrate. The insert shows the layout of the chip.

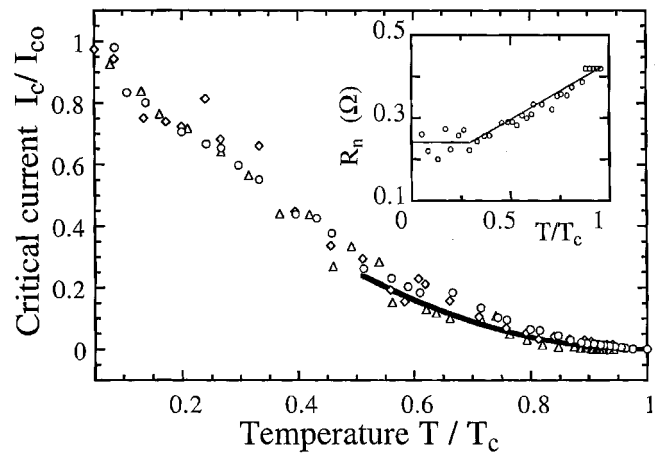


FIG. 3. The temperature dependence of the normalized critical current I_c/I_{c0} for three TI-2212 bicrystal junctions (J_2 , J_3 , and J_5) on one chip. Δ (J_2): 5- μ m-wide junction; \diamond (J_3): 2×5 μ m² dc SQUID; \circ (J_5): 10- μ m-wide junction. The solid line corresponds to $I_c/I_{c0}\propto(1-T/T_c)^2$. The insert shows the temperature dependence of the normal resistance for the junction J_3 . The solid line is a guide to the eye.

crowave power. Shapiro steps up to $n=10$ appeared in the I - V curves at the voltages of $nh\nu/e$ (n is an integer, h is Planck's constant) under microwave radiation with a frequency ν of 10.9 GHz. The dependence of the amplitude of the zeroth and the first steps on the microwave voltage are presented in Fig. 4(b). They can be described by Bessel functions [see the solid lines in Fig. 4(b)]. Some asymmetry and subharmonic phenomena were sometimes observed in the I - V curves. This irregular behavior has not been understood clearly but might be connected to magnetic flux motion in a long Josephson junction. Alternatively, it can be ascribed to nonuniformity of the junction, as suggested in Refs. 14 and 15. We can not distinguish between the two possibilities as we did not systematically study junctions of different widths.

For the best device, the $I_c R_n$ product and the modulation voltage at 77 K were 40 and 16 μ V. The inductance of the

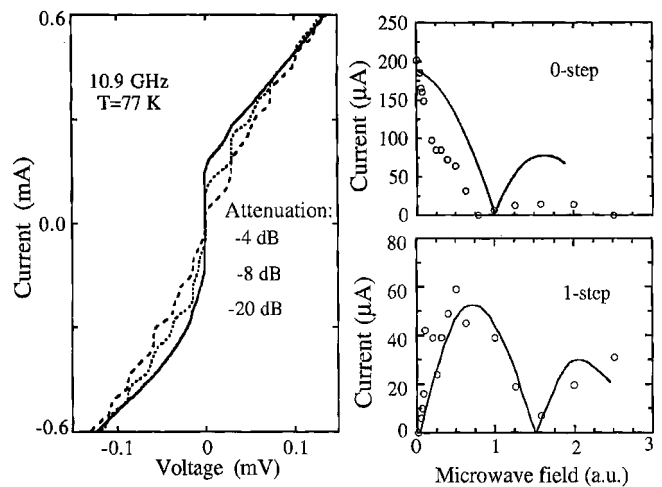


FIG. 4. (a) Shapiro steps in I - V curves of a TI-2212 bicrystal junction under 10.9 GHz microwave radiation at 77 K and three different microwave powers. The amplitudes of the $n=0$ and $n=1$ steps vs microwave voltage are shown in (b); the solid lines are the zeroth and the first Bessel functions.

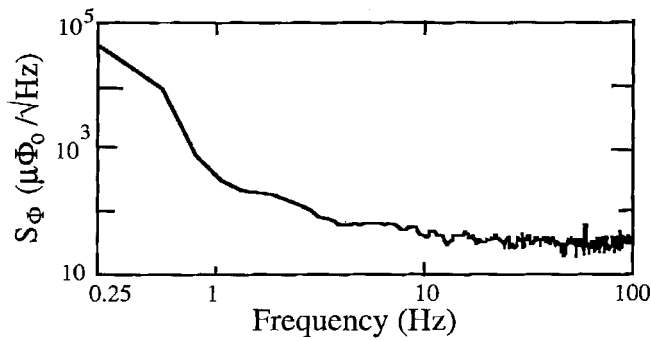


FIG. 5. The optimum flux noise spectrum S_Φ of a Tl-2212 dc SQUID at 77 K recorded in the locked-loop mode and without bias reversing. The transfer function of the device was $32 \mu\text{V}/\Phi_0$. The low-frequency noise started to dominate below about 5 Hz.

SQUID loop was estimated to be 80 pH and the parameter $\beta_L > 1$. The device was flux locked from 77 up to 94 K. The noise spectra of the dc SQUIDs were measured with a standard electronic setup having a noise level of $0.3 \text{ nV}/\sqrt{\text{Hz}}$. This corresponds to a flux noise level of $10 \mu\Phi_0/\sqrt{\text{Hz}}$. The optimum operating bias point for a device could be approached by adjusting the dc bias current of the junction and the applied dc magnetic field. The flux noise spectrum $S_\Phi^\Sigma(f)$ of the measuring system and the frequency response $S_V(f)$ were measured by a HP35663A dynamic analyzer in a locked-loop mode. The transfer function $\partial\Phi/\partial V$ of the instrument was acquired with the shifting of one flux quantum in the output signal by varying the voltage in the input coil. The flux noise spectrum $S_\Phi(f)$ of the dc SQUID was calculated as

$$S_\Phi(f) = \frac{S_\Phi^\Sigma(f)}{S_V(f)} \frac{\partial\Phi}{\partial V}.$$

Figure 5 shows the best flux noise spectrum S_Φ at 77 K, obtained in the locked-loop mode without bias reversing. The white noise level is $50 \mu\Phi_0/\sqrt{\text{Hz}}$. The low-frequency noise dominates below 5 Hz and the noise level at 1 Hz is $440 \mu\Phi_0/\sqrt{\text{Hz}}$. The Tl-2212 dc SQUIDs in the present work may be compared to YBCO dc SQUIDs. The white noise of our devices is several times higher than that of the best YBCO SQUIDs, however, the low-frequency noise level is comparable for the two types of films.

IV. SUMMARY

Tl-2212 weak links and dc SQUIDs made of epitaxial Tl-2212 films on LAO bicrystal substrates with a misorien-

tation angle of 32° were fabricated and studied. The I - V curves of the junctions could be described by a RSJ model without hysteresis. The amplitude of Shapiro steps in the I - V curves oscillate under microwave radiation showing a Bessel function behavior. Close to T_c , the temperature dependence of the critical current of the junctions can be fitted to $(1 - T/T_c)^2$. The characteristics of the junctions indicate that they behave as SNS weak links. The work has shown that Tl-2212 bicrystal dc SQUIDs have rather low $1/f$ noise. At the same time the white noise level does not reach the best values for YBCO devices yet. We believe that the potential of Tl-based SQUIDs should be investigated further.

ACKNOWLEDGMENTS

This work was supported by the Swedish Council of Natural Sciences and by the Consortium of Superconductivity. The Swedish and Chinese Academies of Sciences are acknowledged for support of Y.F.C. The Swedish Nanometer Facility was utilized.

- ¹P. Chaudhari, J. Mannhart, D. Dimos, C. C. Tsuei, J. Chi, M. M. Oprisko, and M. Scheuermann, *Phys. Rev. Lett.* **60**, 1653 (1988).
- ²A. Mistra, Y. Song, P. P. Crooker, and J. R. Gaines, *Appl. Phys. Lett.* **59**, 863 (1991).
- ³K. Char, M. S. Colclough, S. M. Garrison, N. Newman, and G. Zaharchuk, *Appl. Phys. Lett.* **59**, 733 (1991).
- ⁴A. H. Cardona, H. Suzuki, T. Yamashita, K. H. Young, and L. C. Bourne, *Appl. Phys. Lett.* **62**, 411 (1993).
- ⁵R. H. Koch, W. J. Gallagher, B. Oh, and B. Bumble, *Appl. Phys. Lett.* **54**, 951 (1989).
- ⁶V. Foglietti, R. H. Koch, W. J. Gallagher, B. Bumble, and W. Lee, *Appl. Phys. Lett.* **54**, 2259 (1989).
- ⁷Z. G. Ivanov, P. Å. Nilsson, D. Winkler, J. A. Alarco, T. Claeson, E. A. Stepantsov, and A. Ya. Tzalenchuk, *Appl. Phys. Lett.* **59**, 3030 (1991).
- ⁸Z. G. Ivanov, E. Olsson, H. Olin, E. A. Stepantsov, A. Tzalenchuk, T. Claeson, L.-G. Johansson, M. Löfgren, and E. Carlsson, in *Applied Superconductivity*, edited by H. C. Freyhardt (DG Informationsgesellschaft, Göttingen, 1993), Vol. 1, pp. 591–594.
- ⁹E. A. Stepantsov, A.s. 1116100, *Bulleten' izobreteniy-Russia*, No. 36, 1984, p. 77.
- ¹⁰L.-G. Johansson, T. Claeson, Z. G. Ivanov, H. Olin, E. Olsson, and D. Ertz, *J. Supercond.* **7**, 767 (1994).
- ¹¹L.-G. Johansson, V. Langer, E. A. Stepantsov, A. Litvinchuk, L. Börjesson, Y. F. Chen, T. Claeson, Z. G. Ivanov, E. Olsson, and A. Ya. Tzalenchuk, in *EUCAS'95*, *Inst. Phys. Conf. Ser. No. 148* (IOP, Bristol, 1995), Vol. 2, pp. 797–809.
- ¹²P. Å. Nilsson, Z. G. Ivanov, H. K. Olsson, D. Winkler, and T. Claeson, *J. Appl. Phys.* **75**, 7972 (1994).
- ¹³A. H. Cardona, H. Suzuki, T. Yamashita, K. H. Young, and L. C. Bourne, *Appl. Phys. Lett.* **62**, 25 (1993).
- ¹⁴E. A. Early, A. F. Clark, and K. Char, *Appl. Phys. Lett.* **62**, 3357 (1993).
- ¹⁵E. A. Early, R. L. Steiner, A. F. Clark, and K. Char, *Phys. Rev. B* **50**, 9409 (1994).